Catalysis Today xxx (xxxx) xxx–xxx

Contents lists available at ScienceDirect

Catalysis Today

journal homepage: www.elsevier.com/locate/cattod

Theoretical investigation of dephosphorylation of phosphate monoesters on $CeO_2(111)$

Chuanlin Zhao, Ye Xu*

Cain Department of Chemical Engineering, Louisiana State University, Baton Rouge, LA, 70803, USA

ARTICLE INFO

Keywords:
Ceria
Dephosphorylation
Organophosphates
Para-nitrophenyl phosphate
Oxide catalysis
DFT

ABSTRACT

The dephosphorylation of neutral model phosphate monoesters on $CeO_2(111)$, including *para*-nitrophenyl phosphate and methyl phosphate, has been studied theoretically using self-consistent, periodic density functional theory calculations at the GGA + U-PW91 level. These phosphate monoesters interact strongly with $CeO_2(111)$ by forming a bond between the P atom and a surface lattice O atom. A surface-assisted hydrolysis mechanism is proposed for the catalytic dephosphorylation of the phosphate monoesters on $CeO_2(111)$, which involves P-O ester bond scission followed by phosphate hydration and product desorption. The energies of the transition states for the P-O ester bond scission are found to follow a linear scaling relation with respect to the energies of the dissociated fragments reasonably well. A nearly spontaneous transfer of one of the H atoms on the phosphate group to the alkoxide group produces the corresponding alcohol. The hydration of the remaining HPO_3 group has a maximum activation energy of ca. 1.1 eV in vacuo. Thus although the nature of the alkoxide group affects the activation of the P-O ester bond, it should not affect the overall catalytic activity of $CeO_2(111)$ for dephosphorylation because the hydration of the phosphate group is rate-limiting.

1. Introduction

Phosphorous (P) serves as an essential building block for life on earth, and is critical for food production. It has a huge impact on the stability and prosperity of human societies [1]. With the steady growth of global population, primary phosphorus fertilizers necessary for high crop yields have transitioned from animal wastes to mined phosphate rock, i.e., phosphorite. However, phosphorite is a nonrenewable resource and is distributed unevenly from a geographic perspective, and high-grade phosphorite sources are declining [2]. On the other hand, agricultural runoff, industrial wastewater, and human sewage often contains significant amounts of phosphates, which are in part responsible for eutrophication that creates hypoxic dead zones in waterbodies close to shorelines and threatens aquaculture industries but also jeopardizes potable water resources [3]. Furthermore, organophosphates (OPs), which are found in many consumer, industrial, and agricultural chemical products, often possess toxicity to animals and even humans. Removal of P from wastewater as well as extraction of P from biomass feedstock constitutes important steps in sustainable P use [4]. Environmental necessity and economic and technological feasibility of such methods suggest that the further development of and support for sustainable P use need to be on the agenda of policymakers today [5].

The degradation of OPs in the environment can take months and even years [6,7]. The hydrolysis of the P-O ester bond by microbes is the primary pathway for OP degradation in nature [8]. Earlier studies have demonstrated promising catalytic activities of cerium oxide nanoparticles toward aqueous-phase dephosphorylation, i.e. hydrolysis, of organic and biological compounds including phosphopeptides, *para*-nitrophenyl phosphate (*p*-NPP), ATP, and phospho-tyrosine [9,10] that parallel the function of phosphatases. Recently, Janoš et al. suggested that ceria-based reactive sorbents can promote the dephosphorylation of several OP pesticides and chemical warfare agents, which opens up a new frontier for ceria in environmental catalysis and may be relevant to large-scale environmental application of P recovery technologies [11,12]. Manto et al. very recently studied the catalytic dephosphorylation of *p*-NPP using different ceria nano-shapes, among which nano-spheres (ca. 4 nm; no preferential exposed facet) showed the highest catalytic activity, followed by nano-octahedra (ca. 18 nm), which primarily expose (111) facets [13]. Although extensive experimental and theoretical studies have been reported in the literature that examine the hydrolysis mechanism of phosphate esters in aqueous solutions or by enzymatic complexes [14–21], the understanding of the dephosphorylation process on solid surfaces remains incomplete [22–26].

Here we report a DFT + U study on the dephosphorylation of model

---

* Corresponding author.
E-mail address: yexu@lsu.edu (Y. Xu).

https://doi.org/10.1016/j.cattod.2018.02.033
Received 29 November 2017; Received in revised form 14 February 2018; Accepted 21 February 2018

Please cite this article as: Zhao, C., Catalysis Today (2018), https://doi.org/10.1016/j.cattod.2018.02.033

phosphate monoesters, including *p*-NPP and methyl phosphate (MP), on $CeO_2(111)$ in vacuo in order to shed light on the factors controlling the kinetics of this reaction and to help establish the range of OPs the dephosphorylation of which ceria may effectively catalyze under mild or ambient conditions. The OPs are modeled in their neutral forms (PO$(OH)_2$OR) in this work, e.g. *p*-NPP-H_2 and MP-H_2, which are the predominant forms in acidic to neutral conditions [15,27]. The deprotonated forms (i.e., the mono-anionic *p*-NPP-H_1/MP-H_1 and di-anionic *p*-NPP-H_0/MP-H_0) that prevail in neutral to basic solutions [28] will be considered in a future study. The dephosphorylation of *p*-NPP is of interest because it is accompanied by visible color change of the solution, which allows the reaction kinetics to be readily analyzed using ultraviolet-visible (UV–vis) absorption spectroscopy [13]. By comparison, MP is the simplest organic phosphate monoester and is used here to explore how the leaving group affects the activation of the P-O ester bond. Moreover, a linear transition state scaling relation is proposed after considering several additional organic phosphate monoesters, including *para*-chlorophenyl phosphate (*p*-ClPP), phenyl phosphate (*p*-HPP), 2-pyridyl phosphate (2-py-P), and chloro-methyl phosphate (Cl-MP). The formation and desorption of the resulting alcohol species (i.e. *para*-nitrophenol (*p*-NP) or 4-nitrophenol from *p*-NPP, and methanol from MP) are facile and therefore kinetically insignificant. On the other hand, the hydration and desorption of the remaining phosphate group are characterized by activation barriers of ca. 1.1 eV, although they may be reduced in aqueous phase. Our findings thus suggest that the nature of the leaving group should not have a strong impact on the kinetics of dephosphorylation of phosphate monoesters when catalyzed by ceria.

2. Methods

Periodic, spin-polarized DFT calculations were performed using the Vienna Ab initio Simulation Package (VASP) [29] in the generalized gradient approximation (GGA) using the Perdew-Wang (PW91) exchange-correlation functional [30]. The projector-augmented wave method (PAW) was used to describe the core electrons [31], and the Kohn–Sham valence states [Ce(5s5p4f5d6s), Cl(3s3p), P(3s3p), O (2s2p), N(2s2p), C(2s2p), H(1s)] were expanded in a plane wave basis set with a kinetic energy cutoff of 400 eV.

Gas-phase molecules or radicals were optimized in a neutral state in a 15 × 15 × 15 $Å^3$ simulation cell, which has been tested to be sufficiently large for the total energy of *p*-NPP to converge (the minimum-energy gas-phase structures for *p*-NPP and MP are shown in Fig. 1). Dipole decoupling [32] was applied in all three lattice vector directions, and the reciprocal space was sampled at the Γ point only. Gas phase bond energies were calculated as $E_b{}^{A-B} = E_{AB} - E_A - E_B$, where AB, A, and B denotes the parent molecule and the corresponding dissociated fragments, respectively.

The $CeO_2(111)$ surface, which is thermodynamically the most stable facet of ceria, was modeled with a slab consisting of three O—Ce—O tri-layers with a p(3 × 3) surface unit cell, which corresponds to 1/9 monolayer (ML) coverage for one adsorbate per unit cell. The slab was separated from its periodic images in the *z* direction by ca. 12 Å of vacuum. A Γ-centered 2 × 2 × 1 Monkhorst-Pack k-point grid was used to sample the surface Brillouin zone [33]. Adsorption was studied on one side of the slab only, with dipole decoupling in the *z* direction. The top tri-layer of the slab and adsorbate were fully relaxed, and the remaining two tri-layers were fixed at the bulk positions. The adsorption energy of an atom or molecule was calculated as $\Delta E_{ads} = E_{total} - E_{slab} - E_{gas}$, where E_{total}, E_{slab} and E_{gas} refer to the energy of the slab with the adsorbed atom or molecule, the energy of the clean surface, the molecule or radical in the gas phase, respectively. Thus, the more negative the value of ΔE_{ads} is, the stronger the adsorption. The activation energy barrier was calculated as $E_a = E_{TS} - E_{IS}$, where E_{TS}, E_{IS} refer to the energy of transition and initial state of the elementary step, respectively.

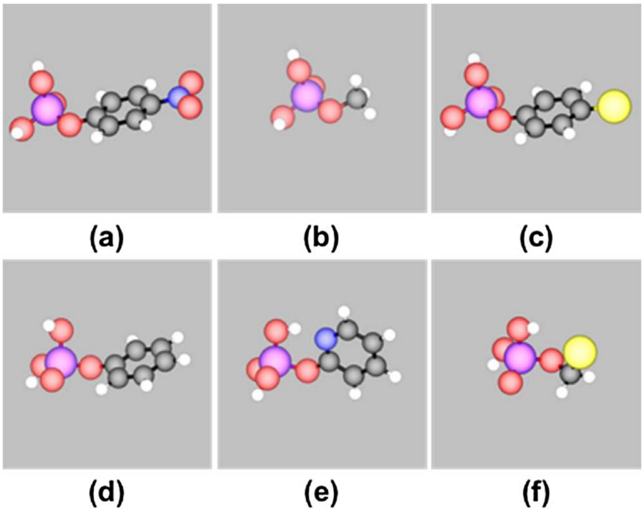

Fig. 1. DFT-calculated minimum-energy gas-phase geometries for: (a) *para*-nitrophenyl phosphate (*p*-NPP); (b) methyl phosphate (MP); (c) *para*-chlorophenyl phosphate (*p*-ClPP); (d) phenyl phosphate (PP); (e) 2-pyridyl phosphate (2-py-P); (f) chloro-methyl phosphate (Cl-MP). Color code (color online): red = O, violet = P, black = C, blue = N, white = H, and yellow = Cl.

The minimum energy reaction path for each proposed elementary step and the associated transition state (TS) were determined using the climbing-image nudged elastic band method [34,35] and dimer method [36,37]. Geometry optimization and transition state search were converged to the extent that the maximum residual force was 0.03 eV/Å and 0.01 eV/Å or less in all relaxed degrees of freedom, respectively. Singlet-triplet/doublet-quadruplet splitting was checked, and the lower adsorption energy for an adsorbate and the lower activation energy for an elementary reaction step (at constant spin) are reported below. Vibrational modes and frequencies were calculated to determine zero point energies (ZPE) and to verify that each transition state possessed only one vibrational mode with a negative curvature in the direction of the bond breaking or forming process. A finite difference approximation approach of the dynamical matrix was used with a displacement of 0.01 Å. Very soft modes below 50 cm^{-1} were replaced with 50 cm^{-1} in calculating ZPEs.

The DFT + U formalism of Dudarev et al. [38] was used to partially offset the 4f electron delocalization error in DFT at the GGA level [39]. A U value of 2 eV was used based on our previous studies of surface reactions of organic oxygenates on $CeO_2(111)$ [40–42]. The equilibrium lattice constant of the CeO_2 bulk was calculated to be 5.476 Å on a (15 × 15 × 15) Monkhorst-Pack k-point grid at U = 2 eV, in close agreement with previous experimental and computational values [43]. Solvation energies of isolated molecules were estimated using the implicit solvation model implemented in VASPsol [44].

3. Results and discussion

In the following, we propose and discuss a surface-assisted hydrolysis mechanism for the dephosphorylation of *p*-NPP. The main surface intermediates involved in this mechanism will be presented first, and then the mechanism and its energy profile, which starts with the adsorption of *p*-NPP, followed by the P—O ester bond scission, the formation and desorption of *p*-NP, the hydration of the remaining phosphate group, and finally the desorption of phosphoric acid (H_3PO_4). A similar pathway is proposed and investigated for MP. Finally, a linear transition state scaling plot is presented for the activation of the P—O ester bond on $CeO_2(111)$ for several additional organic phosphate monoesters together with *p*-NPP and MP.